



NOISE AND SHAPIRO STEP INTERFERENCE IN THE
CHARGE-DENSITY-WAVE CONDUCTOR $K_{0.3}MoO_3$

M.F. Hundley and A. Zettl
Department of Physics, University of California at Berkeley,
Berkeley, CA 94720 USA

(Received 16 December 1987 by A. Zawadowski)

Extremely thin (transverse dimension $\sim 0.2 \mu\text{m}$) samples of the charge density wave (CDW) conductor $K_{0.3}MoO_3$ are found to display unusually coherent narrow-band noise spectra and well defined Shapiro step interference structure. The results suggest an intrinsic pinning potential with periodicity equal to the CDW wavelength. The Shapiro step interference appears to arise from a coupling of the external electric field to the low frequency dielectric relaxation mode rather than to the high frequency pinned phason mode.

The Quasi-one-dimensional material potassium blue bronze ($K_{0.3}MoO_3$) undergoes a Peierls transition at $T_p=180\text{K}$ which leads to the formation of a charge density wave (CDW).^{1,2} The CDW is pinned to the lattice by impurities but can be forced to slide by applying moderate electric fields ($E_p \sim 200\text{mV/cm}$) along the chain axis.³ The sliding CDW state in blue bronze exhibits nonlinear conductivity, broad band noise, and to a limited extent the formation of quasi-periodic [narrow-band noise (NBN)] voltage oscillations.¹ This material also exhibits a low frequency ($<10 \text{ MHz}$), highly temperature dependent, dielectric relaxation mode^{4,5} which appears closely related to a rich metastable state structure.⁶ At high frequencies ($>100 \text{ MHz}$) $K_{0.3}MoO_3$ also displays a pinned conductivity mode analogous to that observed in other "sliding" CDW materials.⁷

Typical blue bronze samples display extremely weak NBN spectra, indicating that the sliding CDW state is very incoherent.¹ In contrast, the CDW material $NbSe_3$ shows highly coherent behavior. $NbSe_3$ grows in fine whiskers with typical dimensions of $1\text{mm} \times 5\mu\text{m} \times 1\mu\text{m}$ (volume = $5 \times 10^{-9} \text{ cm}^3$) whereas a $K_{0.3}MoO_3$ crystal has typical dimensions of $1\text{mm} \times 0.5\text{mm} \times 0.25\text{mm}$ (volume = $1.25 \times 10^{-4} \text{ cm}^3$). If narrow-band noise generation in $K_{0.3}MoO_3$ were a finite size effect, as has been suggested⁸ for $NbSe_3$, then a reduction in crystal volume could be expected to dramatically improve the NBN spectrum quality. Similarly, although no Shapiro step structure has been reported for $K_{0.3}MoO_3$, a sample of sufficiently small volume (and hence high degree of coherence) might be expected to display these ac-dc coupling effects.

In this Communication we report coherent CDW effects in extremely thin samples of potassium blue bronze ($\sim 0.2 \mu\text{m}$ thick, length = 0.625 mm , volume = $6.25 \times 10^{-8} \text{ cm}^3$). We find that these optically transparent samples display exceptionally high quality NBN spectra. We also report the first observation in this material of mode-locked Shapiro steps due to the combined effects of ac and dc fields. These results

provide an accurate means of determining the CDW current density to NBN frequency ratio, and it implies a pinning potential periodicity equal to the CDW wavelength. We analyze the Shapiro step data within the simplest classical approximation and find that the data suggest that external applied electric fields couple to the low frequency screened dielectric relaxation mode rather than to the high frequency pinned phason mode. This is in contrast to Shapiro step interference in $NbSe_3$ and TaS_3 , where the coupling is to the pinned phason mode.

$K_{0.3}MoO_3$ samples were prepared by electrolytic growth from a chemical melt, using platinum electrodes. The samples were then rigidly bound to a sapphire substrate and reduced in size mechanically. Details concerning the cleaving techniques employed to achieve submicron sample thicknesses will be presented elsewhere.⁹ Two probe current driven measurements were performed using evaporated Indium contacts. NBN spectra were measured with an HP8558B spectrum analyzer while the sample differential resistance was measured with a low-frequency lock-in technique. Our experiments were carried out at 77K to facilitate a comparison with previously published results on $K_{0.3}MoO_3$. The extremely fragile crystals were cooled very slowly to 77K to avoid crystal fracture; a He gas flow system provided accurate temperature control.

A typical NBN spectrum obtained from a thin sample of $K_{0.3}MoO_3$ is depicted in Fig. 1. The spectrum shows a sharp fundamental at 80 kHz as well as four higher harmonics. The quality of this NBN spectrum exceeds that of any we or other groups^{3,10,11} have observed in $K_{0.3}MoO_3$ samples of conventional size, which suggests that the sliding CDW state in very thin blue bronze samples is strongly coherent. We note that this behavior is not unique to this sample; all extremely thin (thickness $\leq 1\mu\text{m}$) samples which we have examined display strongly coherent NBN spectra.

In a simple model,¹² the fundamental NBN frequency f_{NBN} is directly proportional to the

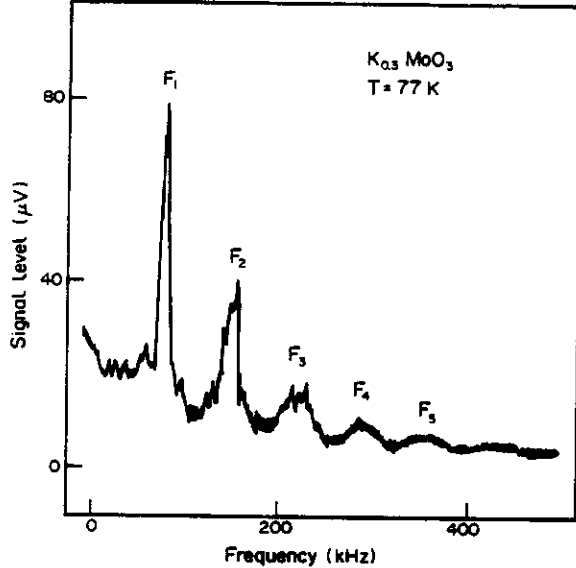


Fig. 1: Narrow band noise spectrum from a thin blue bronze crystal at 77K. The measurement bandwidth is 3 kHz.

excess current density J_{CDW} carried by the CDW condensate:

$$f_{NBN} = \frac{J_{CDW}}{n_c e \lambda} \quad (1)$$

where n_c is the density of CDW carriers and λ is an intrinsic length (taken to be equal to the periodicity of the pinning potential). Eqn. 1 holds for $NbSe_3$ and TaS_3 .^{12,13} There has been some controversy, stemming from low quality NBN spectra and inhomogeneities in CDW current density, as to whether or not Eqn. 1 holds true for $K_{0.3}MoO_3$.^{3,4,10,11}

Our experiments on $K_{0.3}MoO_3$ at 77 K indicate that f_{NBN} is linearly related to J_{CDW} with $f_{NBN}/J_{CDW} = 12 \pm 3$ kHz cm^2/A . With $n_c = 4.95 \times 10^{21} cm^{-3}$ as determined from structural considerations,¹ we thus find from Eqn. 1 $\lambda = 10.6 \pm 2$ Å. This is in good agreement with the CDW wavelength, $\lambda_{CDW} = 9.9$ Å.¹ A similar value has been inferred by NMR measurements.¹⁴

We now consider the combined effects of ac and dc fields. It has been previously demonstrated¹⁵⁻¹⁸ for $NbSe_3$ and TaS_3 that the CDW can be mode locked, resulting in a "Shapiro" step in a sample's differential resistance, whenever the externally applied frequency f_{ex} is related to the internal NBN frequency by

$$p f_{ex} = q f_{NBN} \quad (2)$$

where p and q are integers.¹⁹ The index n of a specific step is given by $n = p/q$. The n th step is said to be a harmonic step if n is an integer, and a subharmonic step otherwise.

The effects of an externally applied ac signal on the differential resistance of a thin blue bronze sample is depicted in Fig. 2. The

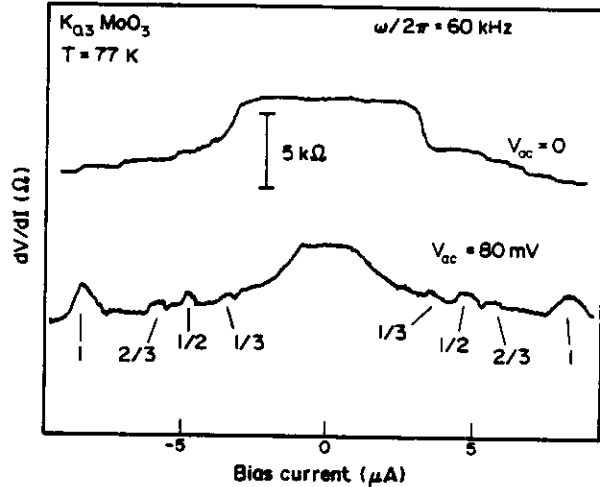


Fig. 2: Ac-dc interference effects in potassium blue bronze. The two traces have been vertically offset for clarity.

top trace shows the sample's current driven differential resistance in the absence of an external ac signal. The curve clearly shows the CDW depinning threshold at $I_T = 2.5 \mu A$ beyond which dV/dI smoothly decreases as the CDW begins to slide. The lower trace shows the effect on the differential resistance when it is measured in the presence of a 60 kHz ac signal with an amplitude $V_{ac} = 4V_T$. This trace shows clear partially mode-locked Shapiro steps which are labeled by their index n in Fig. 2. The first harmonic ($n=1$) as well as three subharmonics ($n=1/3, 1/2$, and $2/3$) are visible in Fig. 2 (note that there is an apparent current polarity dependence to the Shapiro step quality). The large relative height of the mode-locked step indicates that a substantial portion of the CDW condensate is responding coherently.

Shapiro step data provides an independent (and often more accurate) means of determining the NBN frequency to CDW current density ratio. By combining Eqns. 1 and 2 we obtain the following expression for the externally applied frequency to CDW locking current density on step $n = p/q$:

$$\frac{f_{ex}}{J_{CDW}} = \frac{q}{p} \frac{f_{NBN}}{J_{CDW}} = \frac{q}{p} \frac{1}{n_c e \lambda} \quad (3)$$

Plots of the locking current density versus the externally applied locking frequency in $K_{0.3}MoO_3$ at 77 K for $n = 2, 1$, and $1/2$ are depicted in Fig. 3. The NBN frequency versus CDW current density data are also plotted in the figure. The three solid lines correspond to $f_{NBN}/J_{CDW} = 12$ kHz cm^2/A ; hence for all values of n , the mode-locking data give a value for f_{NBN}/J_{CDW} consistent with that extracted from the NBN spectra alone.

Fig. 4 shows the Shapiro step magnitude δV (the area under a Shapiro step in a dV/dI vs. I trace) as a function of the external locking signal amplitude at $f_{ex} = 40$ kHz. δV is a

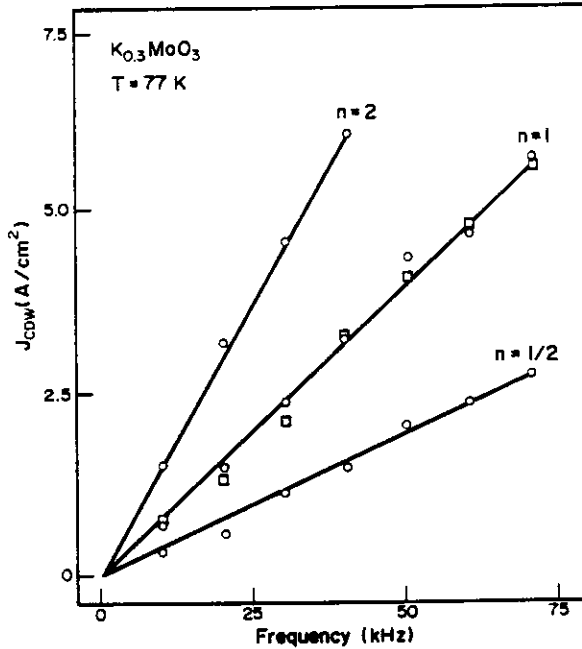


Fig. 3: CDW current density vs. frequency for both Shapiro step (circles) and narrow band noise (squares) data.

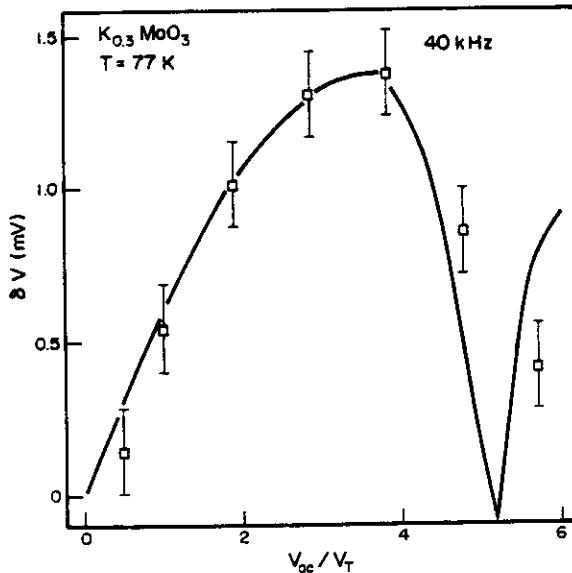


Fig. 4: Shapiro step magnitude δV plotted as a function of the external ac amplitude. The external frequency is set at $f_{ex}=40$ kHz. The solid line is a fit to the data (see text).

strongly varying function of V_{ac} , attaining a maximum value of $\delta V=1.4$ mV at $V_{ac}=4V_T$. The Shapiro step magnitude has also been found to be a strong function of V_{ac} in $NbSe_3$.^{16,18}

The simplest possible equation for CDW transport is one that treats the CDW classically and ignores all internal degrees of freedom:²⁰

$$\frac{d^2 x}{dt^2} + \Gamma \frac{dx}{dt} + \frac{\omega_0^2}{Q} \sin(Qx) = \frac{eE}{m^*}, \quad (4)$$

where x is the CDW center of mass coordinate, $\Gamma=1/\tau$ is a damping coefficient with a relaxation time τ , ω_0 is a characteristic frequency, Q is the pinning potential periodicity, E is the applied electric field, and m^* is the CDW effective mass. With $Q=2k_F=2\pi/\lambda_{CDW}$, Eqn. 1 follows with $\lambda=\lambda_{CDW}$. Eqn. 4 qualitatively and often semi-quantitatively describes CDW transport in $NbSe_3$ and TaS_3 .² It also describes the Shapiro step magnitude dependence on V_{ac} in $NbSe_3$.¹⁶

In the high frequency limit ($f_{ex} \gg \omega_0^2 \tau / 2\pi$), Eqn. 4 predicts¹⁶ for the $n=1$ Shapiro step magnitude

$$\delta V = 2\alpha V_T(\omega=0) |J_1(\beta)|, \quad (5)$$

where α represents the volume fraction locked to the external signal and $\beta = (\omega_0^2 \tau V_{ac} / \omega_{ex} V_T(\omega=0))$. This expression describes the essential qualitative and quantitative features of $\delta V(V_{ac})$ in $NbSe_3$.¹⁶ A more detailed approach changes this theoretical prediction only subtly.¹⁸ In the low frequency (overdamped) limit ($f_{ex} \leq \omega_0^2 \tau / 2\pi$) the inertial term can be neglected, and a modified Bessel-like solution for δV can be obtained numerically.²¹ In the extreme low frequency limit, δV has a maximum at $V_{ac}=V_T$ with an amplitude of $\omega_{ex}/\omega_0^2 \tau$.

A reasonable fit to the data of Fig. 4 can be obtained by using the low frequency solution of ref. 22 and considering $\omega_0^2 \tau$ to be a fitting parameter. The fit in Fig. 4 was thus obtained with $f_0 = \omega_0^2 \tau / 2\pi = 25$ kHz. It is noteworthy that this value is four orders of magnitude below the characteristic frequency of the high frequency pinned mode seen in $K_{0.3}MoO_3$ ($\omega_0^2 \tau / 2\pi \approx 500$ MHz),⁷ while it is in the frequency range of the low frequency dielectric relaxation mode of $K_{0.3}MoO_3$.⁴ Low frequency (0.1 kHz - 1000 kHz) ac conductivity measurements⁹ on the sample of Figs. 1-4 indicate a rise in the conductivity beginning at $f \approx 20$ kHz. Because the contribution to δV from the 500 MHz mode is expected to be negligible at $f_{ex}=40$ kHz [$\delta V(f_0=500 \text{ MHz})/\delta V(\text{measured})=10^3$], it appears that the ac-dc interference effects here observed in $K_{0.3}MoO_3$ are a direct result of interactions with the low frequency dielectric relaxation mode.

We consider in more detail the low temperature behavior of blue bronze which gives rise to low frequency Shapiro steps. The typical NBN frequencies in $K_{0.3}MoO_3$ are very low, in the 10 to 100 kHz range. In addition, CDW motion is highly damped below 100 K, with the CDW conductivity at $E \gg E_T$ roughly equal to the normal carrier ohmic conductivity.²² The NBN frequency and dc conductivity predicted by Eqn. 4 are

$$f_{NBN} = \frac{1}{2\pi} \frac{Q \tau e}{m^*} E g(E), \quad (6)$$

and

$$\sigma_{dc}(E) = \frac{n e^2 \tau}{m^*} g(E), \quad (7)$$

respectively, where $g(E)$ is a function of the applied electric field [$g(E < E_T) = 0$, $g(E > E_T) = 1$]. Eqns. 6 and 7 indicate that within the context of a simplified classical model, low values for f_{NBN} and σ_{dc} indicate large CDW damping (small τ). Hence, a small value of the fundamental resonance frequency $\omega_0 \tau$ is a direct result of large CDW damping below 100 K.

An estimate for $f_0 = \omega_0 \tau / 2\pi$ can be obtained by combining the electric threshold field $E_T = m \omega_0^2 / Qe$ with the high field limit of Eqn. 7:

$$f_0 = \left(\frac{f_{NBN}}{J_{CDW}} \right) \sigma_{dc}(E \gg E_T) E_T. \quad (8)$$

For the sample considered here [$f_{NBN}/J_{CDW} = 12$ kHz cm^2/A , $E_T = 320$ mV/cm, and $\sigma_{dc}(E \gg E_T) = 10$ (Ωcm) $^{-1}$], Eqn. 8 predicts a fundamental resonance frequency $f_0 = 44$ kHz, in reasonable order-of-magnitude agreement with the frequencies determined from both the fit to the Shapiro step data and from the ac conductivity measurement. This again argues for ac-dc coupling to the dielectric relaxation mode, rather than to the pinned phason mode in $K_{0.3}MoO_3$. The presence of two independent modes in $K_{0.3}MoO_3$ has been discussed by Littlewood.²³ In the low frequency (<10 MHz) limit, normal electrons effectively screen²⁴ the moving CDW, leading to an

enhancement in CDW damping and the creation of an overdamped low frequency pinned mode. In the high frequency (>100 MHz) limit, normal electrons are ineffective in damping CDW motion and an additional, unscreened and underdamped high frequency pinned mode is realized. The Shapiro step data presented here provides direct evidence that these two modes are qualitatively very similar in that externally applied ac and dc fields can couple to both modes.

We briefly consider the possibility of coupling to the high frequency (~500 MHz) pinned mode in $K_{0.3}MoO_3$. This would require performing a mode locking experiment at roughly $f_{ex} \sim 100$ MHz, necessitating CDW currents three orders of magnitude larger [$I_{CDW}(f_{NBN} = 100$ MHz) ~ 1 mA] than those used in the experiments discussed here. Due to the large resistance (~ 10 k Ω at 77 K) of the thin samples which display strongly coherent NBN features, Joule heating with a typical power of ~ 10 mW would make a conventional dc-biased Shapiro step experiment impractical. The high frequency mode might be observable by performing a pulsed mode locking experiment.

We thank M.F. Crommie, P. Parilla, and M.S. Sherwin for useful discussions. This research was supported by NSF Grant No. DMR 84-00041. One of us (A.Z.) acknowledges support from the Alfred P. Sloan Foundation.

References

1. C. Schlenker in "Low Dimensional Conductors and Superconductors", Series B, Vol. 155, D. Jérôme and L.G. Caron, eds. (Plenum Press, New York, 1987) p. 477.
2. for a review see G. Grüner and A. Zettl, Physics Reports 119,117 (1985).
3. J. Dumas, C. Schlenker, J. Marcus, and R. Buder, Phys. Rev. Lett. 50,757 (1983), and J. Dumas and C. Schlenker, Solid State Commun. 45,885 (1983).
4. R.J. Cava, R.M. Fleming, P. Littlewood, E.A. Rietman, L.F. Schneemeyer, and R.G. Dunn, Phys. Rev. B 30, 3228 (1984).
5. R.P. Hall, M.S. Sherwin, and A. Zettl, Solid State Commun. 54, 683 (1985).
6. for a review of metastable effects in $K_{0.3}MoO_3$ see R.M. Fleming in ref. 1, p. 433.
7. D. Reagor and G. Mozurkewich (unpublished), also G. Mihály, J. Dumas, and A. Jánossy, Solid State Commun. 60, 785 (1986).
8. G. Mozurkewich and G. Grüner, Phys. Rev. Lett. 51, 2206 (1983).
9. M.F. Hundley and A. Zettl (to be published).
10. A. Jánossy, G. Kriza, S. Pekker, and K. Kamarás, Europhys. Lett. 3, 1027 (1987).
11. G. Mihály and P. Beauchêne, Solid State Commun. 63, 911 (1987).
12. F. Monceau, J. Richard, and M. Renard, Phys. Rev. Lett. 45, 43 (1980).
13. A. Zettl and G. Grüner, Phys. Rev. B 28, 2091 (1983).
14. P. Ségransan, A. Jánossy, C. Berthier, J. Marcus, and P. Butand, Phys. Rev. Lett. 56, 1854 (1986).
15. P. Monceau, J. Richard, and M. Renard, Phys. Rev. B 25, 931 (1982).
16. A. Zettl and G. Grüner, Solid State Commun. 46, 501 (1983), and Phys. Rev. B 29, 755 (1984).
17. S.E. Brown, G. Mozurkewich, and G. Grüner, Solid State Commun. 54, 23 (1985).
18. R.E. Thorne, W. G. Lyons, J.W. Lyding, and J.R. Tucker, Phys. Rev. B 35, 6360 (1987).
19. S.E. Brown, G. Mozurkewich, and G. Grüner, Phys. Rev. Lett. 52, 2277 (1984).
20. G. Grüner, A. Zawadowski, and P.M. Chaikin, Phys. Rev. Lett. 46, 511 (1981).
21. H. Fack and V. Kose, J. Appl. Phys. 42, 320 (1971).
22. R.M. Fleming, R.J. Cava, L.F. Schneemeyer, E.A. Rietman, and R.G. Dunn, Phys. Rev. B 33, 5450 (1986).
23. P.B. Littlewood, Phys. Rev. B 36, 3108 (1987).
24. L. Sneddon, Phys. Rev. B 29, 719 (1984).